Generating Cadastral Maps from Aerial Photos of Rural Areas

Wonho Song, South Korea

Key words: Artificial Intelligence, conditional GAN, Cadastral map, Aerial Photography, Rural Area

SUMMARY

In the field of image processing, various image-processing methods have been used to extract objects or boundaries in images. Before 2012, problems were usually solved by image processing technic itself, but after that, they started to solve the problems using deep learning. Recently, more complex deep learning methods have been used to produce excellent results close to the intended ones. However, due to the complex nature of geospatial objects and obstacles such as moving objects or shadows etc., extraction of objects or semantic segmentation in images is usually not satisfactory. And there are few studies using deep learning in the cadastral field.

In this study, we uses a conditional GAN and automatically generates a cadastral map. cGAN is a deep neural network model, and we uses images acquired from airborne in rural areas in this study. ResNet-9 and ResNet-101 were used to increase the computational efficiency of conditional GAN. The images used for processing are 7612 pieces of training data and 1903 pieces of test data set, with a total of about 9515 images. The study area includes Bucheon, Seongnam, Yeoju, Icheon, and Pyeongtaek cities, which are near the Seoul metropolitan area.

The training used cadastral maps and images acquired from the airborne and generated trained model. The trained model create a cadastral map from the image dataset. We investigate the loss function on the cGAN model. (BCE vs MSE), the ResNet-9 and ResNet-101 constructors, PatchGAN and ImageGAN discriminator. And the Performance is quantitatively evaluated by MSE evaluation indicators.

As summary, ResNet-9 with BCE has the best performance. In addition, the result is not better just because the network is deeper. We need to carefully adjust the model to prevent the mode collapse and no learning in the future.

The research shows that deep learning has a potential in many image translation problems.

Generating Cadastral Maps from Aerial Photos of Rural Areas (11403)
Wonho Song (Republic of Korea)

FIG Congress 2022
Volunteering for the future - Geospatial excellence for a better living
Warsaw, Poland, 11–15 September 2022

Generating Cadastral Maps from Aerial Photos of Rural Areas

Wonho Song, South Korea

1. Introduction

A map shows the state of a part or whole of the earth's surface on a plane by reducing it to a certain ratio using promised symbols or characters, and there are various types of maps such as military maps, administrative maps, and cadastral maps depending on the purpose.

The cadastral map of South Korea is a map showing the ownership of land, and the boundary registered in the map indicates the scope of ownership.

Surveying or investigation is a main tool to make maps. Surveying refers to the technique of determining the relative position of all points on the earth's surface and measuring the position, shape, area, etc.

On the other hand, remote sensing is a means of indirect surveying that measures an object remotely, and in a small sense, it refers to the technology of observing the earth's surface with satellites or aircraft.

It was difficult to produce the desired level of maps automatically from the images acquired by remote sensing. These images has its own characteristics, such as weather, shadow, unidentified object, resolution, and number of channels and so on.

Entering the 21st century, the wind of the fourth industrial revolution is blowing, and artificial intelligence is currently booming due to the development of Internet and computer technology. Artificial intelligence is a very effective tool in image processing fields such as segmentation and object detection. In fact, deep learning shows better results than existing image processing technology in many computer vision problems.

CNNs and GANs have become commonly used tools for these various image processing and prediction problems.

In particular, since GAN learns loss adaptive to data, GAN could use for various tasks that require different types of loss functions.

The cGAN (Conditional Generative Adversarial Network) model is one of a general solution of the image translation task, and there are many GAN features to improve the performance of the image translation result. (Tang et al., 2020).

2. Literature reviews

In 2014, Eigen et al. [22] first conducted a study using CNN for images. In the study, it proposes a method to increase translation accuracy by using a scale-invariant loss function, but in a method such as CNN, the loss function plays a very important role, which determines the weight of the convolution filter.

The development of generative adversarial networks provided a new perspective on image transformation. Isola et al. [4] proposed that the network adapt to the task and data by learning

---

Generating Cadastral Maps from Aerial Photos of Rural Areas (11403)
Wonho Song (Republic of Korea)

FIG Congress 2022
Volunteering for the future - Geospatial excellence for a better living
Warsaw, Poland, 11–15 September 2022

a loss function using a conditional adversarial network for a wide range of image transformation tasks. This method was meaningful in that it can provide a general solution without manipulating parameters in the image conversion operation.

Mehdi Mirza [2] introduced an adversarial generative network specifying conditions on both the generator and discriminator so that simply providing data y is enough to build a model. This allowed the model to generate MNIST numbers conditional on class labels.

Phillip Isola [12] studied conditional adversarial networks as general-purpose solutions for image translation. This study learns a mapping between inputs and outputs, but also learns a loss function to train this mapping. Using this has the potential in various image-processing fields through learning loss function without parameter adjustment.
.
In addition, cGAN applied in various fields. He Zhang [10] conducted a deraining experiment to remove rain from images using cGAN. Grigory Antipov [7] conducted an experiment related to facial aging using cGAN. Runde Li [17] conducted a dehazing experiment to remove fog from images using cGAN. Emily Denton [15] introduced a simple semi-supervised learning approach for images using adversarial loss. She created an image with random patches removed with a generator that fills in holes according to surrounding pixels. Vu Nguyen [16] conducted a study to detect shadows in images using cGAN.

Jiayi Ma [3] proposed a novel end-to-end model called dual discriminant conditionally generated adversarial network (DDcGAN) to fuse infrared and visible images of different resolutions. In addition to the content, the two discriminators aim to distinguish the structural differences between the fused image and the two source images, respectively. As a result, the fused image must simultaneously retain the thermal radiation of the infrared image and the texture details of the visible image.

Riaz Ullah Khan [6] evaluated the performance of the ResNet model on two different datasets to evaluate the performance of the ResNet model. The first dataset consisted of images for medical data, and the second dataset consisted of malicious code and benign files to predict cancer in the first dataset and detect malware in the second dataset.

Mohammad Sadegh Ebrahimi [18] designed a ResNet model that can perform simple image classification tasks on the Tiny ImageNet data set. This ResNet model compared with the equivalent ConvNet (ConvNet) by removing the residual connections to check the performance. We showed that ResNet tends to overfit despite the higher accuracy, which can depend on the depth of the network. We found that several methods to prevent overfitting, such as adding a dropout layer and a stochastic increase in the training data set, can attenuate this problem in ResNet.

Yu Li [1] proposes an asymmetric GAN (AsymGAN) for asymmetric adaptation with the goal of unpaired image transformation, and introduces an auxiliary variable (aux) to learn

Generating Cadastral Maps from Aerial Photos of Rural Areas (11403)
Wonho Song (Republic of Korea)

FIG Congress 2022
Volunteering for the future - Geospatial excellence for a better living
Warsaw, Poland, 11–15 September 2022

information between two domains by one-to-many mapping of different amounts of information between domains.

Laxman, [5] performed high-resolution image conversion using Multi-Scale Gradient U-Net.

Abbas Jafar [9] built a hyperparameter optimization approach for ResNet models and took a manual search approach. Compared to the previous automated approach, this improves the error rate greatly and reduces computing time. Jafar, A [9] performed high-speed hyperparameter optimization for image recognition using deep ResNet models.

In this study, image conversion performed to automatically recognize cadastral boundaries from aerial images and generate cadastral maps using conditional GAN. The conditional GAN learns a model conditioned on input images and generates output images. As a generator, ResNet-9 model shows the best results so far. ResNet-101 is a deeper version of ResNet. So that this study applied and compared these two models. In order to judge the effect of the loss function, it compares the BCE loss and the MSE loss.
As a discriminator, PatchGAN has excellent performance and uses small resources. ImageGAN is a method of scoring the entire image. This study applied and compared these two models too. For quantitative evaluation of the translated image, it uses MSE (Mean Squared Error).

The main goals of this study are:
• Test the loss function on the cGAN model. (BCE vs MSE)
• Test the constructors ResNet-9 and ResNet-101.
• Test discriminator PatchGAN and ImageGAN.

• Performance is quantitatively evaluated by MSE indicators.

3. Preperation

3.1 Dataset

Data sets are half-meter-level aerial photographs of areas below and corresponding cadastral maps. The specifications of the aerial photograph are as follows.

Table 1 Aerial Datasets

Images	Y1	X1	Y2	X2	Band	X Resol	Y Resol
Gunpo	193046.79	525032.36	197579.29	530683.36	X: 9065 Y: 11302 Band: 3	0.500000	- 0.500000
Bucheon	177578.93	541691.20	184329.93	550132.20	X: 13502 Y: 16882 Band: 3	0.500000	-0.500000
Sungnam	210749.83	536136.98	215283.33	541793.98	X: 9067 Y: 11314 Band: 3	0.500000	- 0.500000
Yeoju	235179.13	403919.51	268051.39	437707.28	X: 65744 Y: 67575 Band: 3	0.500004	- 0.500004
Icheon	228694.65	391536.55	257781.88	430492.85	X: 58174 Y: 77912 Band: 3	0.500004	- 0.500004
PyoungTack	179845.23	377560.94	215563.02	405412.67	X: 71435 Y: 55703 Band: 3	0.500004	- 0.500004

Generating Cadastral Maps from Aerial Photos of Rural Areas (11403)
Wonho Song (Republic of Korea)

FIG Congress 2022
Volunteering for the future - Geospatial excellence for a better living
Warsaw, Poland, 11–15 September 2022

Cadastral map

In general, demarcation and segmentation of boundaries in an image depends on image characteristics. Therefore, when it extracts the boundary from the image, there is a high possibility of extracting natural boundary. On the other hand, the boundary of the cadastral map in Korea is a boundary set by law, and there are special boundary rules that do not coincide with natural boundaries. The figure below shows the boundaries of the cadastral map.
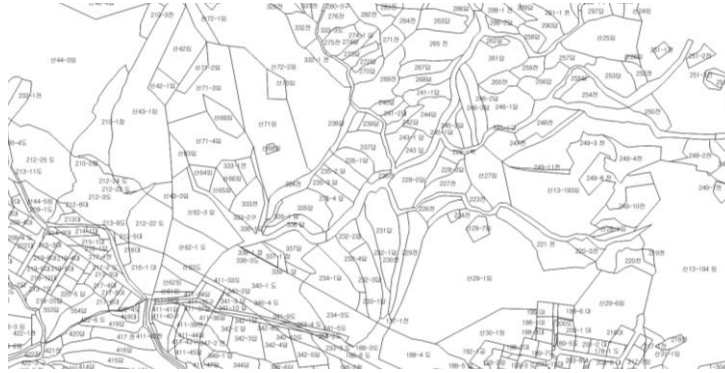

Figure 1 Cadastral map in South Korea

As for the dataset, it splits the dataset into the 80% of training dataset and the 20% of validation dataset in rural areas, respectively. Number of images is about 9.5 thousand in rural areas. The images are the RGB channel images.

Table 2 Data preperation

Study Area	Epoch	Sum	80%	20%	Cities
Rural	100	9,515	7,612	1,903	Bucheon, Yeoju, Icheon ,PyoungTack

3.2 Hardware and Software

The computer specification is as follows.
1. CPU i7, Graphic GTX 1660, RAM 16G
2. CPU i5, Graphic GTX 1060 3G, RAM 8G

Software's installed are Python, Tensorflow, PyTorch, etc. Each epoch generates a checkpoint to check the detail checkpoint status. The processing time using GPU was about 30 minutes per epoch.

4. Methods

cGAN is a composed model of generator G and discriminator D. This model learns the mapping from input image x to output image y, G: x → y. Adversarially trained discriminator D discriminates authenticity Generator G. Figure 1 is the illustration of conditional GAN

Generating Cadastral Maps from Aerial Photos of Rural Areas (11403)
Wonho Song (Republic of Korea)

FIG Congress 2022
Volunteering for the future - Geospatial excellence for a better living
Warsaw, Poland, 11–15 September 2022

architecture. As training continues by the G and D, the converted image gradually becomes closer to original image.
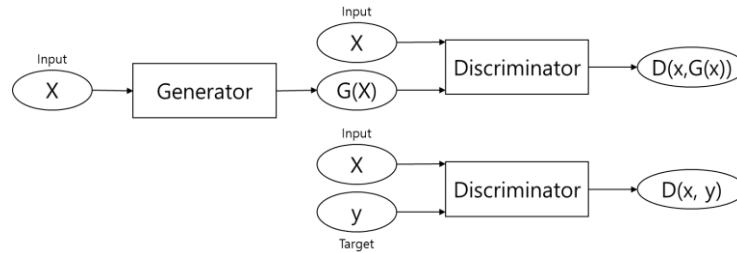

Figure 2 cGAN architecture

4.1 Preprocessing

Original image size is too big. Small one is about 10000 x 10000, and bigger one is about 70000 x 6000. So that we divide it into 256 x 256 tiles. After that, resize the input image to 286 x 286 for the random cropping and did normalization.

4.2 Training

We use Mini-batch SGD and ADAM solver optimizer. Hyper-parameters are below.
- batch size to 1
- dropout ratio to 0.5
- learning rate of 0.0002
- GAN loss to BCE or MSE
- G model is ResNet-9 or ResNet-101
- D model is PatchGAN or ImageGAN

Each model runs 100 epochs.

We use ResNet-9 generator, which has good performance in many reviews. In addition, we use ResNet-101 to check deeper residual network.

4.3 Loss function verification (BCE vs MSE)

Choosing a loss function is a very important aspect of GAN model design. The GAN loss function is an adversarial loss function that calculates the distance between the GAN distribution of the generated data and the distribution of the actual data. All GAN models have two loss functions. One is to train a generator network and the other is to train a discriminator network. These two-loss functions works together to form an adversarial loss function. (Tzeng et al., 2017).

The loss of CGAN consists of two parts: adversarial loss and L1 loss. The loss can be expressed as $\mathcal{L}_{cGAN}(G,D) = E_{x,y}[\log D(x,y)] + E_x[\log(1 - D(x,G(x)))]$.

Generating Cadastral Maps from Aerial Photos of Rural Areas (11403)
Wonho Song (Republic of Korea)

FIG Congress 2022
Volunteering for the future - Geospatial excellence for a better living
Warsaw, Poland, 11–15 September 2022

Compared to the L2 distance, the Ll distance moderately ignores outliers and add to the generator loss to sharpen the low-frequency image. So the target function is $(G^*, D^*) = \arg\min_G \max_D \left(\mathcal{L}_{cGAN}(G,D) + \lambda \mathcal{L}_{L1}(G) \right)$.

MSE loss
The definition of mean square error loss is just calculate the difference between the value from the output node and the desired target value. Squared error value is always positive. The MSE is the mean of these squared errors.

$$\text{MSE} = \frac{1}{n}\sum_{i=1}^{n}(o - t)^2$$

Where n: each node of the output layer, o: output, t: target value.

The reason why the result of the discriminator is 0.5 means that it is impossible to determine whether the data is generated or genuine with the same size.

BCE loss
Binary cross entropy loss depends on probability and uncertainty. Cross entropy is defined as the amount of information that one event X has for two probability distributions p and q. That is, the amount of information the same event has for two different probability distributions is calculated. BCE is a special case of cross entropy for the task of predicting one of two classes.

$$\text{BCE} = -\frac{1}{n}\sum_{j=1}^{n}\sum_{i=1}^{c}[y_i \log(p_i) + (1 - y_i)\log(1 - p_i)]]$$

Where y: actual class label (0 or 1), p: predicted probability for class, c: number of classes, n: number of samples.

For the loss function, MSE and BCE were tested.

4.4 Network architecture verification

4.4.1 Generator network (ResNet-9 vs ResNet-101)

Sometimes the deeper the layer of the model, the worse the performance occurs, because of the gradient vanishing / exploding problem. Gradient vanishing means that the degree of weight that affects the output becomes smaller as the layer deepens, and the differential value becomes smaller even after back propagation because the differentiation increases more and more.
ResNet solved this problem of gradient vanishing as the layer deepens through residual learning using skip connection.
It uses ResNet-9 and ResNet-101 models using residual-based networks in this study.
ResNet-9's network consists of 2 encoding blocks, 9 residual blocks and 2 decoding blocks. Each encoding or decoding block follows the 2-stride convolution/deconvolution-

Generating Cadastral Maps from Aerial Photos of Rural Areas (11403)
Wonho Song (Republic of Korea)

FIG Congress 2022
Volunteering for the future - Geospatial excellence for a better living
Warsaw, Poland, 11–15 September 2022

InstanceNorm-ReLU structure, and each residual block follows the convolution-InstanceNorm-ReLU-convolution-InstanceNorm Residual connection structure.

Both generators process an input image x of size 3 x 256 x 256 and produce an output image G(x) of the same size. Repeat the steps of gradient descent for G and D alternately during training. We use the cross-entropy loss (BCE) and discriminant loss for the adversarial loss. This transformation is

$$\mathcal{L}_{gen}(G, D) = BCE\ or\ MSE\left(D\big(x, G(x)\big), 1\right) + \lambda \mathcal{L}_{L1}(G)$$
$$\mathcal{L}_{dis}(G, D) = BCE\ or\ MSE\left(D\big(x, G(x)\big), 0\right) + BCE\ or\ MSE(D(x, y), 1)$$

4.4.2   Discriminator network (PatchGAN vs ImageGAN)

The discriminator used PatchGAN classifier network. The PatchGAN discriminator uses a local patch of 70 x 70 size rather than the entire image to determine whether an image is real or fake. In addition, since the sliding window passes through the small image patch unit, the number of parameters is much smaller, so the operation speed is faster. Since it is not depends on the overall image size, it is also flexible from a structural point of view. The discriminator takes two images, an input image (x) and an unknown image (G(x) or y), passes them through 5 downsampling convolutional-BatchNorm-LeakyReLU layers, and outputs a 30 x 30 matrix. One element corresponds to the classification of one patch.

The optimization target function of the generator includes the L1 loss, which has a direction to minimize the Euclidean distance between the original image and the generated image, so it tends to focus on the average component of the image, which is the low frequency. Because the L1 loss covers the low-frequency region, the discriminator can focus on the high-frequency component (detail) and determine whether it is real/fake. In a typical GAN structure, it gets a score for the entire image, which is ImageGAN.

ImageGAN is useful for cloud removal, which is an essential step to enhance the quality of cloud-covered remote sensing image. ImageGAN is effective to focus on global information for thick cloud-covered images. [21]

5. Result

5.1 Visual analysis

Experimental results show that ResNet-9 generators can capture common features of aerial images while ResNet-101 falls into mode collapse. ResNet-9 produces clearer road definitions. We are expecting ResNet-101 with deeper network layers produces better results but it was not. ResNet-101could not find the overall data distribution and gives a weight to only one mode.

Below shows, 11 sample images and the generated map images of the both architectures. ResNet-9 with BCE(Binary Cross Entropy) is the best result. ResNet-9 with ImageGAN Discriminator has the second result because ImageGAN only judge the whole image distribution at once while PatchGAN check details with local distribution. Third is the MSE that uses a L2 loss. The exponential L2 value is more sensitive than the Euclidian L1 value.

Generating Cadastral Maps from Aerial Photos of Rural Areas (11403)
Wonho Song (Republic of Korea)

FIG Congress 2022
Volunteering for the future - Geospatial excellence for a better living
Warsaw, Poland, 11–15 September 2022

Figure 3 Visual analysis

5.2 Model evaluation

The evaluation uses the mean square error (MSE) per pixel between the generated image and the original cadastral map image.

$$\text{MSE} = \frac{1}{w \cdot h} \sum_{j=1}^{h} \sum_{i=1}^{w} (O_{ij} - T_{ij})^2$$

MSE is smaller, the better. The following table shows the mean square error (MSE) observed for two different generator networks. ResNet-9 with BCE has the lowest MSE, so we can assume that it is closest to the real thing.
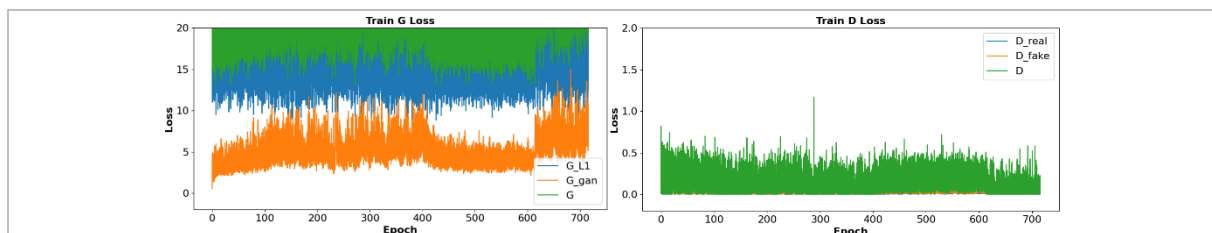
Generating Cadastral Maps from Aerial Photos of Rural Areas (11403)
Wonho Song (Republic of Korea)

FIG Congress 2022
Volunteering for the future - Geospatial excellence for a better living
Warsaw, Poland, 11–15 September 2022

Table 3 MSE results

| Image No	RenNet-9			ResNet-101
	BCE	MSE	ImageGAN	BCE/MSE/ImageGAN
Average	1263.855	1685.744	1352.507	2039.539
1	1343.072	2115.19	1433.135	2333.292
2	641.1027	1709.467	1143.234	1988.268
3	840.6652	1396.481	631.1481	1819.789
4	1546.08	2724.162	2503.745	3376.895
5	1974.294	1428.981	1599.517	1770.283
6	607.7222	1936.426	820.6284	1506.057
7	728.2318	1694.259	718.7419	2036.222
8	503.2178	697.509	1323.413	972.0905
9	1079.648	554.9541	634.3876	793.6936
10	503.0614	673.9441	681.1909	877.7407
11	4135.313	3611.812	3388.435	4960.598

5.3 Discriminator Score

It is difficult to train GAN well. Figure below shows the generator and discriminant Loss of the ResNet-9 and Resnet-101 that occurred while the model was training from the beginning to the 100th epoch. It says G and D seem to converge well. In particular, G is stably adapted between epoch 70~80, and D also converges to 0.5 in epoch 70~80. Therefore, we use a checkpoint in epoch 70~80. After epoch 90, overfitting seems to have occurred.
Below shows the training loss of ResNet-9 with BCE.

Below shows, the training loss of ResNet-9 with MSE, which did not trained at all.
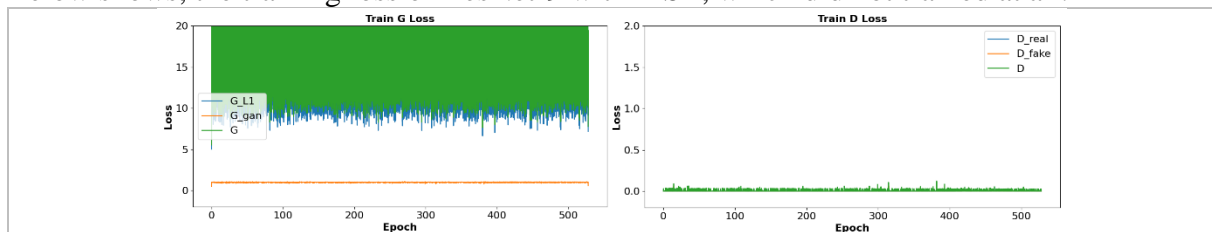
5.4 Result

The main results are:

Generating Cadastral Maps from Aerial Photos of Rural Areas (11403)
Wonho Song (Republic of Korea)

FIG Congress 2022
Volunteering for the future - Geospatial excellence for a better living
Warsaw, Poland, 11–15 September 2022

- Test the loss function on the cGAN model. (BCE vs MSE)
    - The BCE, which uses the L1 loss, is much better than the MSE.
- Test the constructors ResNet-9 and ResNet-101.
    - The ResNet-9-based GAN model has much better performance compared to the ResNet-101-based GAN model in the quality results and the visual analysis.
- Test discriminator PatchGAN and ImageGAN.
    - The PatchGAN discriminator is better than the ImageGAN discriminator.

- Performance is quantitatively evaluated by MSE evaluation indicators.
    - Indicator says that ResNet-9 with BCE model has the best value.

6. Conclusion

Conditional adversarial networks are a promising approach for many image transformation tasks. It can apply the network to a variety of settings by learning the appropriate loss for the given data and the required task. In other words, C-GAN becomes an effective solution for transforming images from one visual domain to another.

In our study, we first generated a model using the ResNet-9 and ResNet-101 architecture. Moreover, we compared the generated results using the both architecture. ResNet-9 based generator model improved the performance compared to the ResNet-101 based generator model.

The experimental result is.
1. The BCE, which uses the L1 loss, is much better than the MSE.
2. The ResNet-9-based GAN model has much better performance compared to the ResNet-101-based GAN model in the quality results and the visual analysis.
3. The PatchGAN discriminator is better than the ImageGAN discriminator.
4. Indicator says that ResNet-9 with BCE model has the best value.

For the future, we need to investigate more on BN(Batch Normalization), ReLU, Unrolling GANs, DCGANS, ResNet-6 and so on. In addition, the datasets as drone image is the candidate to experiment. Most important thing is the dataset itself. To ensure better generalization of the network, refine and enriches the datasets.

Generating Cadastral Maps from Aerial Photos of Rural Areas (11403)
Wonho Song (Republic of Korea)

FIG Congress 2022
Volunteering for the future - Geospatial excellence for a better living
Warsaw, Poland, 11–15 September 2022

REFERENCES

1. Li, Y. et al. Asymmetric GAN for Unpaired Image-to-image Translation. CoRR abs/1912.11660, (2019).
2. Mirza, M. & Osindero, S. Conditional Generative Adversarial Nets. CoRR abs/1411.1784, (2014).
3. J. Ma, H. Xu, J. Jiang, X. Mei, & X. -P. Zhang. DDcGAN: A Dual-Discriminator Conditional Generative Adversarial Network for Multi-Resolution Image Fusion. IEEE Transactions on Image Processing 29, 4980–4995 (2020).
4. He, K., Zhang, X., Ren, S. & Sun, J. Deep Residual Learning for Image Recognition. CoRR abs/1512.03385, (2015).
5. Laxman, K., Dubey, S. R., Kalyan, B. & Kojjarapu, S. R. V. Efficient High-Resolution Image-to-Image Translation using Multi-Scale Gradient U-Net. arXiv:2105.13067 [cs, eess] (2021).
6. Khan, R. U., Zhang, X., Kumar, R. & Aboagye, E. O. Evaluating the Performance of ResNet Model Based on Image Recognition. in Proceedings of the 2018 International Conference on Computing and Artificial Intelligence 86–90 (Association for Computing Machinery, 2018). doi:10.1145/3194452.3194461.
7. G. Antipov, M. Baccouche, & J. Dugelay. Face aging with conditional generative adversarial networks. in 2017 IEEE International Conference on Image Processing (ICIP) 2089–2093 (2017). doi:10.1109/ICIP.2017.8296650.
8. Goodfellow, I. J. et al. Generative Adversarial Networks. arXiv:1406.2661 [cs, stat] (2014).
9. Jafar, A. & Lee, M. High-speed hyperparameter optimization for deep ResNet models in image recognition. Cluster Comput (2021) doi:10.1007/s10586-021-03284-6.
10. H. Zhang, V. Sindagi, & V. M. Patel. Image De-Raining Using a Conditional Generative Adversarial Network. IEEE Transactions on Circuits and Systems for Video Technology 30, 3943–3956 (2020).
11. Gao, H., Chen, Z., Huang, B., Chen, J. & Li, Z. Image super-resolution based on conditional generative adversarial network. IET Image Processing 14, 3006–3013 (2020).
12. Isola, P., Zhu, J.-Y., Zhou, T. & Efros, A. A. Image-to-Image Translation with Conditional Adversarial Networks. CoRR abs/1611.07004, (2016).
13. Wang, C., Xu, C., Wang, C. & Tao, D. Perceptual Adversarial Networks for Image-to-Image Transformation. CoRR abs/1706.09138, (2017).
14. Zhao, Y., Gao, H., Guo, P. & Sun, Z. ResiDualGAN: Resize-Residual DualGAN for Cross-Domain Remote Sensing Images Semantic Segmentation. CoRR abs/2201.11523, (2022).
15. Denton, E., Gross, S. & Fergus, R. Semi-Supervised Learning with Context-Conditional Generative Adversarial Networks. arXiv:1611.06430 [cs] (2016).

Generating Cadastral Maps from Aerial Photos of Rural Areas (11403)
Wonho Song (Republic of Korea)

FIG Congress 2022
Volunteering for the future - Geospatial excellence for a better living
Warsaw, Poland, 11–15 September 2022

16.Nguyen, V., Vicente, T. F. Y., Zhao, M., Hoai, M. & Samaras, D. Shadow Detection with Conditional Generative Adversarial Networks. in 2017 IEEE International Conference on Computer Vision (ICCV) 4520–4528 (IEEE, 2017). doi:10.1109/ICCV.2017.483.

17.Li, R., Pan, J., Li, Z. & Tang, J. Single Image Dehazing via Conditional Generative Adversarial Network. in 2018 IEEE/CVF Conference on Computer Vision and Pattern Recognition 8202–8211 (IEEE, 2018). doi:10.1109/CVPR.2018.00856.

18.Ebrahimi, M. S. & Abadi, H. K. Study of Residual Networks for Image Recognition. in Intelligent Computing (ed. Arai, K.) 754–763 (Springer International Publishing, 2021).

19.Abu-Srhan, A., Abushariah, M. A. M. & Al-Kadi, O. S. The effect of loss function on conditional generative adversarial networks. Journal of King Saud University - Computer and Information Sciences (2022) doi:10.1016/j.jksuci.2022.02.018.

20.Liu, M.-Y., Breuel, T. & Kautz, J. Unsupervised Image-to-Image Translation Networks. 9.

21.X. Wang, G. Xu, Y. Wang, D. Lin, P. Li and X. Lin, "Thin and Thick Cloud Removal on Remote Sensing Image by Conditional Generative Adversarial Network," IGARSS 2019 - 2019 IEEE International Geoscience and Remote Sensing Symposium, 2019, pp. 1426-1429, doi: 10.1109/IGARSS.2019.8897958.

22. Eigen, D., Puhrsch, C., & Fergus, R. 2014, Depth map prediction from a single image using a multi-scale deep network, in Advances in Neural Information Processing Systems, Cambridge, MA, Dec 2014, pp.2366-2374. doi:10.5555/2969033.2969091

BIOGRAPHICAL NOTES

CONTACTS

Mr. Wonho Song
LX Education Institute
182 Yeonsudanji-gil, Sagok-myeon, Gongju-si, Chungcheongnam-do, South Korea (32522)
Gongju
South Korea
Tel. +82 10 2237 6469
Email: whsong@lx.or.kr
Web site: www.lx.or.kr

Generating Cadastral Maps from Aerial Photos of Rural Areas (11403)
Wonho Song (Republic of Korea)

FIG Congress 2022
Volunteering for the future - Geospatial excellence for a better living
Warsaw, Poland, 11–15 September 2022